

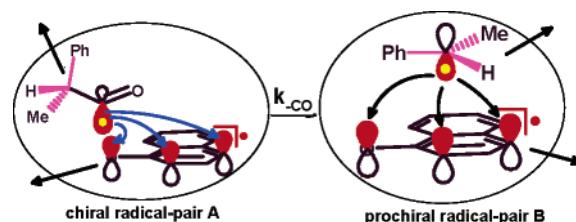
Analyses of In-Cage Singlet Radical-Pair Motions from Irradiations of 1-Naphthyl (*R*)-1-Phenylethyl Ether and 1-Naphthyl (*R*)-2-Phenylpropanoate in *n*-Alkanes

Jinqi Xu and Richard G. Weiss\*

Department of Chemistry, Georgetown University, Washington, D.C. 20057-1227

weissr@georgetown.edu

Received October 14, 2004



The regio- and stereochemistries of photo-Claisen reactions of 1-naphthyl (*R*)-1-phenylethyl ether ((*R*)-**2**), in combination with photo-Fries and photo-Claisen-type reactions of 1-naphthyl (*R*)-2-phenylpropanoate ((*R*)-**1**), have been investigated in *n*-alkanes of different viscosities and at several temperatures. Analyses of the results provide detailed information about the in-cage motions of the singlet prochiral 1-naphthoxy/1-phenylethyl radical pairs (radical-pair **B**) that are formed directly from (*R*)-**2** and indirectly from (*R*)-**1** via decarbonylation of singlet chiral 1-naphthoxy/2-phenylpropanoyl radical pairs (radical-pair **A**). In hexane at 23 °C, the photo-Claisen products from irradiations of (*R*)-**2** retain up to 31% enantiomeric excess (*ee*), but the *ees* of the same photoproducts from (*R*)-**1** are near 0%. This disparity is attributed to differences between the initial orientations of the constituent radicals of radical-pair **B** at the moment of their “birth”. The regio- and stereoselectivities reach plateau values as the solvent viscosity increases, indicating that the relationships between the rates of radical–radical bond formation and either translational or tumbling motions within a solvent cage reach an asymptotic limit. Detailed analyses are presented of the various motions that are in competition within a solvent cage during the very short lifetimes of the radical pairs. The data, in toto, present interesting insights into how radical pairs move during short periods and over short distances when their solvent cages have walls of varying flexibility.

## Introduction

Stereochemical information can offer unique insights into how radical-pair combinations occur in isotropic solutions.<sup>1</sup> The chemical course of such combinations can be mediated by the polarity and viscosity of the solvent,<sup>2</sup> as well as by the method of formation and spin multiplicity of the radical pair.<sup>3</sup> Because reorientational motions of a radical are rapid in nonviscous media, little retention

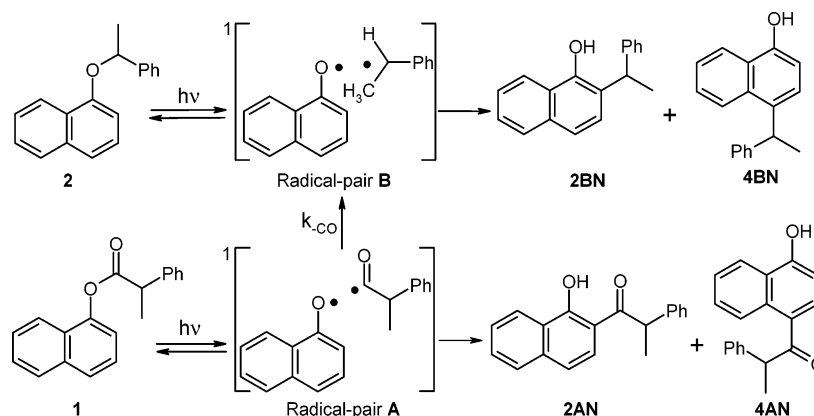
of original stereochemistry is generally observed during radical-pair combinations when a small molecule (such as N<sub>2</sub> or CO<sub>2</sub>) is expelled between the radicals as a nonconcerted step along the pathway leading to their formation,<sup>1</sup> or the radical pair is formed in a triplet state and must undergo intersystem crossing before combining. However, some triplet radical-pair combinations do proceed with high retention of configuration in very constrained anisotropic environments,<sup>4</sup> and others occur even in low-viscosity isotropic solvents.<sup>3</sup> The information obtained from assessing stereochemistry and medium properties provides interesting insights into the combination processes.<sup>4–6</sup>

(1) (a) Curran, D. P.; Porter, N. A.; Giese, B. *Stereochemistry of Radical Reactions: Concepts, Guidelines, and Synthetic Applications*; VCH: Weinheim, Germany, 1995; pp 242–250 and references therein. (b) John, L. E. *An Introduction to Free Radicals*; Wiley: New York, 1993; pp 56–76 and references therein.

(2) (a) Koenig, T.; Owens, J. M. *J. Am. Chem. Soc.* **1973**, *95*, 8484–8486. (b) Koenig, T.; Owens, J. M. *J. Am. Chem. Soc.* **1974**, *96*, 4052–4054. (c) Gao, F.; Boyles, D.; Sullivan, R.; Compton, R. N.; Pagni, R. M. *J. Org. Chem.* **2002**, *67*, 9361–9367.

(3) (a) Bhanthumnavin, W.; Arif, A. M.; Bentrude, W. G. *J. Org. Chem.* **1998**, *63*, 7753–7758. (b) Bhanthumnavin, W.; Bentrude, W. G. *J. Org. Chem.* **2001**, *66*, 980–990.

## SCHEME 1



Previously, we have found that singlet 1-naphthoxy/1-phenylethyl radical pairs (radical-pair **B** in Scheme 1) are produced *indirectly* upon irradiation of 1-naphthyl 2-phenylpropanoate (**1**), after decarbonylation of the initially formed 2-phenylpropanoyl radicals of the singlet 1-naphthoxy/2-phenylpropanoyl radical pairs (radical-pair **A**).<sup>7</sup> In-cage combinations of radical-pair **A** lead to reformation of **1** and to photo-Fries rearrangement products, 1-[2-(1-hydroxynaphthyl)]-2-phenyl-1-propanone (**2AN**) and 1-[4-(1-hydroxynaphthyl)]-2-phenyl-1-propanone (**4AN**) (Scheme 1). Analogous in-cage combinations of radical-pair **B** produce 1-naphthyl 1-phenylethyl ether (**2**), 2-(1-phenylethyl)-1-naphthol (**2BN**), and 4-(1-phenylethyl)-1-naphthol (**4BN**).<sup>7,8</sup> The ca. 24-ns time constant at 23 °C for expulsion of CO from a 2-phenylpropanoyl radical in isotropic media of low polarity<sup>9</sup> allows radical-pairs **B** to lose much of the orientational information originally within their precursors, radical-pairs **A**, immediately after lysis of the excited singlet state of **1**. The *direct* formation of radical-pair **A** and

*indirect* formation of radical-pair **B** contribute to their very different regiochemical fates.

However, radical-pair **B**<sup>7c,8,10,11</sup> can be formed directly by photo-Claisen reactions of **2**, allowing it to be born with orientational information like that of radical-pair **A**. Here, we investigate both the regiochemical and stereochemical consequences of producing *prochiral* radical-pair **B** upon irradiations of the (*R*)-enantiomer of **2**, in the liquid phases of *n*-alkanes (ranging from *n*-hexane to *n*-heptadecane). These results are compared with the fates of radical-pair **B** (as well as radical-pair **A**) generated upon irradiation of the (*R*)-enantiomer of **1**, (*R*)-**1**,<sup>12</sup> and the in-cage and out-of-cage components of radical-pair **B** are separated.

The enantiomeric excesses (*ees*) of the **2BN** and **4BN** photoproducts (and **2** when (*R*)-**1** is the reactant) formed in-cage are influenced by, among other factors, (1) the relative rates of rotation and diffusion of the radicals; (2) the distance the radical center of the 1-phenylethyl radical must traverse from its initial position (when the O–C bond of **2** is lysed or the carbonyl group of 2-phenylpropanoyl of radical-pair **A** is lost) to each of the positions of the 1-naphthoxy radical where it combines; and (3) the ease with which the radical pairs can adopt a spatial orientation conducive to bond formation at the O, C(2), and C(4) positions of the 1-naphthoxy radicals. The distances increase in the order O < C(2) < C(4), but the spin densities on a 1-naphthoxy radical (and, therefore, the propensity to form a bond with 1-phenylethyl) increase in the order O < C(2) < C(4).<sup>7c,13</sup> Both the regio- and stereoselectivities of photoreactions of (*R*)-**2** reach plateau values as the solvent viscosity increases, indicating that the relationships between the rates of radical–radical bond formation and either translational or tumbling motions within a solvent cage reach an asymptotic limit.

The body of data provides detailed information about the motions of the radical pairs within their original

(4) (a) Step, E. N.; Tarasov, V. F.; Buchachenko, A. L.; Turro, N. J. *J. Phys. Chem.* **1993**, *97*, 363–373. (b) Turro, N. J. *Chem. Commun.* **2002**, 2279–2293. (c) Warriar, M.; Turro, N. J.; Ramamurthy, V. *Tetrahedron Lett.* **2000**, *41*, 7163–7167. (d) Choi, T.; Peterfy, K.; Khan, S. I.; Garcia-Garibay, M. A. *J. Am. Chem. Soc.* **1996**, *118*, 12477–12478. (e) Ellison, M. E.; Ng, D.; Dang, H.; Garcia-Garibay, M. A. *Org. Lett.* **2003**, *5*, 2531–2534. (f) *Photochemistry in Organized and Constrained Media*; Ramamurthy, V., Ed.; VCH: New York, 1991. (g) *Photochemistry of Organic Molecules in Isotropic and Anisotropic Media*; Ramamurthy, V.; Schanze, K. S., Eds.; Marcel Dekker: New York, 2003.

(5) Lewis, F. D.; Magyar, J. G. *J. Am. Chem. Soc.* **1973**, *95*, 5973–5976.

(6) Lee, K. W.; Horowitz, N.; Ware, J.; Singer, L. A. *J. Am. Chem. Soc.* **1977**, *99*, 2622–2627.

(7) (a) Gu, W.; Warriar, M.; Ramamurthy, V.; Weiss, R. G. *J. Am. Chem. Soc.* **1999**, *121*, 9467–9468. (b) Gu, W.; Weiss, R. G. *Tetrahedron* **2000**, *56*, 6913–6925. (c) Gu, W.; Weiss, R. G. *J. Photochem. Photobiol., C: Photochem. Rev.* **2001**, *2*, 117–137, and references therein.

(8) For comprehensive reviews, see (a) Miranda, M. A.; Galindo, F. In *Photochemistry of Organic Molecules in Isotropic and Anisotropic Media*; Ramamurthy, V.; Schanze, K. S., Eds.; Marcel Dekker: New York, 2003; Chapter 2. (b) Miranda, M. A. In *Handbook of Organic Photochemistry and Photobiology*; Horspool, W. M., Song, P. S., Eds.; CRC Press: Boca Raton, FL, 1995; pp 570–578. (c) Miranda, M. A.; Galindo, F. In *Handbook of Organic Photochemistry and Photobiology*, 2nd ed.; Horspool, W. M., Lenci, F., Eds.; CRC Press: Boca Raton, FL, 2003; Chapter 42.

(9) The rate of decarbonylation of a 2-phenylpropanoyl radical in alkane media appears to be independent of medium viscosity. (a) Turro, N. J.; Gould, I. R.; Baretz, B. H. *J. Phys. Chem.* **1983**, *87*, 531–532. (b) Lunazzi, L.; Ingold, K. U.; Scaiano, J. C. *J. Phys. Chem.* **1983**, *87*, 529–530. (c) Zhang, X.; Nau, W. M. *J. Phys. Org. Chem.* **2000**, *13*, 634–639. (d) Tsentelovich, Y. P.; Fischer, H. *J. Chem. Soc., Perkin Trans. 2* **1994**, *4*, 729–733.

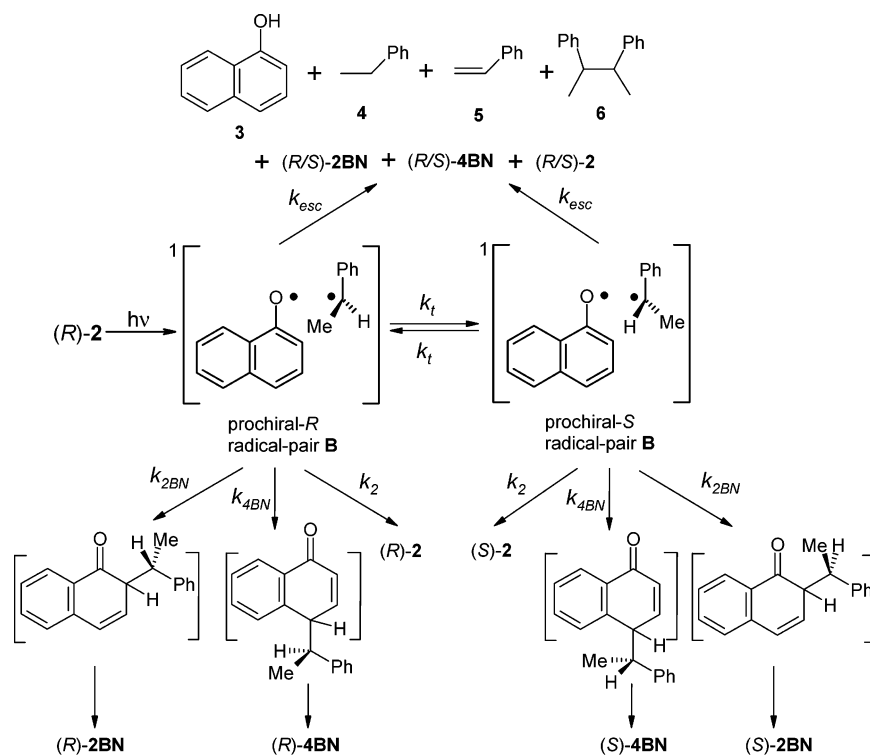
(10) The photo-Claisen chemistry of a similar compound, benzyl 1-naphthyl ether,<sup>10a</sup> has been studied in detail in various media. (a) Gu, W.; Warriar, M.; Schoon, B.; Ramamurthy, V.; Weiss, R. G. *Langmuir* **2000**, *16*, 6977–6981.

(11) In hexane, the quantum yield for cleavage from the triplet state of benzyl 1-naphthyl ether upon direct irradiation is <0.01 while that from its singlet state is ca. 0.12.<sup>7c,10</sup>

(12) Xu, J.; Weiss, R. G. *Org. Lett.* **2003**, *5*, 3077–3080.

(13) (a) Gu, W.; Weiss, R. G. *J. Org. Chem.* **2001**, *66*, 1775–1780. (b) Dixon, W. T.; Foster, W. E. J.; Murphy, D. J. *Chem. Soc., Perkin Trans. 2* **1973**, *15*, 2124–2127.

## SCHEME 2



solvent cages and demonstrates the importance of the interplay between time and viscosity in the retention (or loss) of orientational “memory” by the constituent radicals. Whereas radical-pair **B** from lysis of **2** is formed in a specific orientation that can be related to its ether precursor, radical-pair **B** from lysis of **1** and then decarbonylation of radical-pair **A** retains little or no memory of the shape of the ester. The ability to follow both the regiochemistry and stereochemistry of radical-pair **B** in-cage reactions makes the irradiations of (*R*)-**2**, especially in combination with those of (*R*)-**1**, a very informative probe system of local motions by radical pairs during short periods.

## Results

**Combinations of Radical-Pairs A and B in *n*-Alkanes.** Both the  $(2\text{BN}/4\text{BN})_{\text{total}}$ <sup>14</sup> product ratios and  $ee_{\text{total}}$  of the remaining **2** vary with its degree of photoconversion in hexane at 23 °C (Figure S1 of Supporting Information). The presence of a significant amount of (*S*)-**2** at higher conversions of (*R*)-**2** requires that both enantiomers be considered in analyses of the reactions, including those dealing with the kinetics. Furthermore, secondary photoreactions of **2BN** and **4BN**<sup>15</sup> or of their keto precursors prior to tautomerization<sup>12,16</sup> can also

complicate analyses. However, at conversions approaching 0%, the amount of (*S*)-**2** and secondary photoproducts are mechanistically inconsequential. Therefore, the relative yields in hexane and the other media reported in Table 1 have been extrapolated to 0% conversion of (*R*)-**2** using linear regressions of data from conversions in the range of 2–30% (see Supporting Information). The extrapolated *ee* values for **2BN** and **4BN** are predicted from analyses of Scheme 2 to be the same. The fact that they are not demonstrates that even Scheme 2 does not encompass the total complexity of the radical-pair **B** motions. Despite these shortcomings, we have not included additional steps in the scheme as a compromise between rigor and conceptual understanding.

The degree of racemization of (*R*)-**2** at different conversions has also been analyzed<sup>17</sup> to calculate *S*, the efficiency of photoracemization due to recombination of radical-pair **B**, using eq 1, where  $ee_{(R)\text{-}2}$  is 99.5%, the enantiomeric excess of (*R*)-**2** before irradiation. The *S* values from the slopes of plots in Figure 1 for all of the *n*-alkanes and at both 23 and 60 °C, from 0.13 to 0.16, are probably the same within the limits of experimental error.

$$S = \ln(ee_{2\text{-total}}/ee_{(R)\text{-}2})/\ln(1 - \text{conversion fraction}) \quad (1)$$

In hexane at 23 °C, the relative product yields from **1** are constant to ca. 30% conversions<sup>7</sup> and the photoproduct ratios are ca. 1.9 for  $(2\text{AN}/4\text{AN})_{\text{total}}$  and  $\approx 1.0/1.4/4.0$  for  $(2/2\text{BN}/4\text{BN})_{\text{total}}$  (Table 1 and Table S1 of Supporting Information).<sup>19</sup> The enantiomeric excesses of the decar-

(14) “Total” indicates the observed values from radical-pair combinations; “in-cage” refers to the values from in-cage combinations of radical pairs as calculated (vide infra).

(15) Both **2BN** and **4BN** have strong absorbances at ca. 280–320 nm (i.e., within the wavelength region of irradiation). Control experiments demonstrate that (1) photolysis of **2BN** produces a small amount (ca. 10%) of **4BN** and other compounds, but **4BN** does not generate **2BN**; (2) the disappearance rate of **2BN** is much faster than that of **4BN** when their mixture is irradiated at >300 nm.

(16) (a) Jiménez M. C.; Miranda, M. A.; Scaiano J. C.; Tormos, R. *Chem. Commun.* **1997**, 1487–1488. (b) Mori, T.; Takamoto, M.; Saito, H.; Furo, T.; Wada, T.; Inoue, Y. *Chem. Lett.* **2004**, 33, 256–257.

(17) (a) Tarasov, V. F.; Shkrob, I. A.; Step, E. N.; Buchachenko, A. L. *Chem. Phys.* **1989**, 135, 391–404. (b) Tarasov, V. F.; Ghatlia, N. D.; Buchachenko, A.; Turro, N. J. *J. Phys. Chem.* **1991**, 95, 10220–10229.

TABLE 1. Radical-Pair B Combinations from Irradiations of (*R*)-2 in the Liquid Phases of Various *n*-Alkanes<sup>a,b</sup>

medium	<i>T</i> (°C)	viscosity <sup>c</sup> ( $\eta$ ; cP)	microviscosity <sup>d</sup> ( $\eta_m$ ; cP)	% <i>ee</i> <sub>2BN</sub>		% <i>ee</i> <sub>4BN</sub>		2BN <sup>e</sup>		4BN <sup>e</sup>		2BN/4BN <sup>f</sup>		(2 × ( <i>S</i> )-2 + 2BN + 4BN) <sub>in-cage</sub> <sup>g</sup>	
				total	in-cage	total	in-cage	total	in-cage	total	in-cage	6 <sup>e</sup>	total		in-cage
hexane	23	0.3036	0.1811	31	33	18	21	28.6	26.5	46.1	40.1	4.8	0.62	0.66	71
hexane <sup>b</sup>	23	0.3036	0.1811	1		<1		4.3		12.3		7.5	0.35		
hexane	60	0.2223	0.1389	27	30	16	19	26.2	23.4	44.4	36.5	6.3	0.59	0.64	64
decane	23	0.8926	0.3941	39	41	23	26	31.8	30.5	41.2	37.6	2.9	0.77	0.81	74
decane	60	0.5517	0.2527	36	37	22	23	27.9	26.8	43.0	39.9	2.5	0.65	0.67	74
tetradecane	23	2.198	0.8258	48	50	32	34	36.7	35.6	42.2	39.3	<2.4 <sup>i</sup>	0.87	0.91	81
tetradecane	60	1.154	0.4443	41	42	27	29	32.7	31.6	43.6	40.6	<2.5 <sup>i</sup>	0.75	0.78	78
heptadecane	23	3.907	1.364	47	48	32	33	37.3	36.6	43.2	41.2	<1.6	0.87	0.89	84

<sup>a</sup> “Total” indicates the observed value; “in-cage” refers to product from *in-cage* combinations of radical-pair **B** as calculated from “total” yields using eqs S1–S14 in Supporting Information and as explained in the Discussion Section. The “total” (i.e., observed) *ees* of photoproducts and 2BN/4BN product ratios from irradiations of (*R*)-2 are extrapolated values to 0% conversion. <sup>b</sup> *Ees* of (*R*)-1 and (*R*)-2 before irradiation were 99.5%. The experimental error in *ee* determinations was  $\pm 1.0\%$ . <sup>c</sup> From ref 18. <sup>d</sup> See ref 40. <sup>e</sup> Entries refer to relative yields (%) based on the sum of 2BN, 4BN, **3**, **5**, and **6**. <sup>f</sup>  $\pm 0.02$ . <sup>g</sup> Entries refer to relative yields (%) based on the sum of 2 × (*S*)-2, 2BN, 4BN, **3**, **5**, and **6**; they are lower limits to *in-cage* combination yields from radical-pair **B**. <sup>h</sup> Reactant is (*R*)-1; the relative yields of the other products, 2AN, 4AN, and **2**, are 43.0%, 22.8%, and 3.1%, respectively; *ee*<sub>2</sub> is 1%; details are included in Table S1 of Supporting Information. <sup>i</sup> Approximate values based on  $[6/(2BN + 4BN)]_{\text{total}} = 0.03$ .

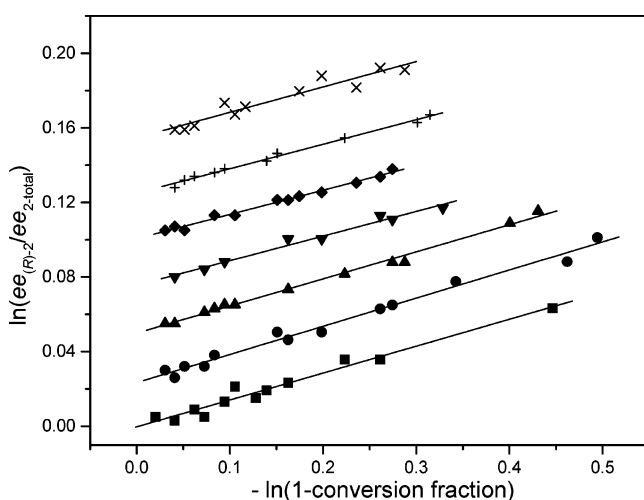


FIGURE 1. Plots of  $\ln(ee_{(R)-2}/ee_{2\text{-total}})$  versus  $-\ln(1 - \text{conversion fraction})$  for irradiations of (*R*)-2 in hexane at 23 °C (■) and 60 °C (●), in decane at 23 °C (▲) and 60 °C (▼), in tetradecane at 23 °C (◆) and 60 °C (+), and in heptadecane at 60 °C (×). Points at each plot from bottom to top are vertically offset by 0.025 increments for clarity.

bonylated products are near 0%, and their relative product distribution mirrors the relative spin densities of the 1-naphthoxy radical: (O < C(2) < C(4)).<sup>13</sup> The (2BN/4BN)<sub>total</sub> product ratio (a measure of the regioselectivity of radical-pair **B** combinations) is somewhat smaller from (*R*)-1 (ca. 0.35) than from (*R*)-2 (ca. 0.62). A lower ratio from (*R*)-1 is expected if its radical-pair **B** has lost much of the memory of the initial spatial disposition of radical-pair **A** at the moment it loses a molecule of CO. Additionally, a relatively large amount of 2,3-diphenylbutane (**6**),<sup>20</sup> a product derived only from *out-of-cage* combinations (i.e., from radicals that escape from their original cages and encounter other radicals

(18) *Physico-Chemical Constants of Pure Organic Compounds*; Timmermans, J., Ed.; Elsevier: New York, 1965; Vol. 2.

(19) Additional information on the product distribution from irradiations of (*R*)-1 in hexane is summarized in Table S1 of Supporting Information.

(20) Product **6** from irradiations of racemic **1** is a mixture of *meso*- and (*d, l*)-isomers.<sup>7</sup> We have not investigated the *ee* of **6** from (*R*)-1 but suspect that it is racemic as well.

subsequently), is detected upon irradiations of (*R*)-1. The stereoselectivities and yields of **6** are consistent with the trends in regioselectivities: the 31% *ee*<sub>2BN-total</sub> and 18% *ee*<sub>4BN-total</sub> from irradiations of (*R*)-2 (i.e., from directly formed radical-pairs **B** and assuming enrichment of the (*R*)-enantiomers<sup>21</sup>) dwarf the negligible values for the same products from irradiations of (*R*)-1; the ca. 4.8% relative yield of **6** from irradiations of (*R*)-2 suggests that these combinations involve more *in-cage* and less *out-of-cage* processes than when (*R*)-1 is irradiated.

The photo-Claisen reactions of (*R*)-2 were also investigated in the liquid phases of *n*-alkanes more viscous than hexane. (2BN/4BN)<sub>total</sub> product ratios increase with viscosity at 23 °C, while the amount of **6** decreases from ca. 4.8% in hexane to <1.6% in heptadecane. Concurrently, the stereoselectivity of radical-pair **B** combinations is enhanced: *ees*<sub>total</sub> of 2BN and 4BN are 47% and 32%, respectively, in heptadecane. These results indicate that virtually all of the 2BN and 4BN is formed by combinations of radical-pairs **B** from (*R*)-2 that remain in their original cages in the higher viscosity *n*-alkanes.

As expected, (2BN/4BN)<sub>total</sub> and *ees*<sub>total</sub> from irradiations of (*R*)-2 are lower at 60 °C than at 23 °C in each of the solvents (Table 1). Plots of these parameters (Figure 2) demonstrate that the changes are induced by viscosity and reach limiting (plateau) values at  $\geq 2.5$  cP.

**Optimized Geometries of 2 in its S<sub>0</sub> and S<sub>1</sub> Electronic States.** Pertinent structural parameters of the optimized geometries of **2** in its S<sub>0</sub> and S<sub>1</sub> electronic states are presented in Table 2. The global-energy minimized conformation, **2-G**, and one local minimum, **2-L**, in the ground state were located through optimization of **2**, starting from several initial geometries with different C(2)–C(1)–O(11)–C(12) dihedral angles, and they were used as initial structures in excited-state calculations (Figure 3). The calculated energy differences between the **2-G** and **2-L** conformers are 12.6 kJ/mol (by B3LYP/6-31G\*) in their S<sub>0</sub> state and 8.8 kJ/mol (by CIS/6-31G\*) in their S<sub>1</sub> state. These correspond to Boltzmann popula-

(21) This assumption is supported by the following evidence: (a) product **2** derived from prochiral radical-pairs **B** of (*R*)-1 in various polyethylene films<sup>12</sup> contains an excess of the (*R*)-enantiomer; (b) the retention times of the larger peak of the separated enantiomer of 2BN and 4BN in their chiral HPLC chromatograms are the same for irradiations of (*R*)-1 in polyethylene films<sup>12</sup> and for (*R*)-2 in *n*-alkanes.

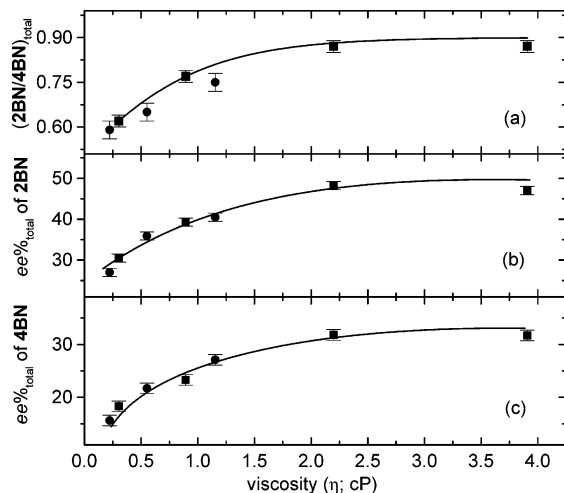


**FIGURE 2.** Plots of (a)  $(2\text{BN}/4\text{BN})_{\text{total}}$ , (b)  $ee\%_{\text{total}}$  of **2BN**, and (c)  $ee\%_{\text{total}}$  of **4BN** from irradiations of (*R*)-**2** at 23 (■) or 60 °C (●) versus bulk viscosity ( $\eta$ ) of various *n*-alkanes. The curves are intended as visual aids and do not derive from a physical model.

**TABLE 2.** Pertinent Structural Parameters of Optimized Geometries for the **2-G** and **2-L** Conformations of **2** in Its  $S_0$  and  $S_1$  Electronic States

states	2-G		2-L	
	$S_0$	$S_1$	$S_0$	$S_1$
C(2)–C(1)–O(11)–C(12) angle <sup>a</sup>	–10.5°	–12.4°	98.3°	101.8°
C(1)–O(11) (Å)	1.352	1.347	1.363	1.358
O(11)–C(12) (Å)	1.411	1.413	1.422	1.424

<sup>a</sup> A positive dihedral angle is defined when sighting along the C(1)–O(11) bond as a clockwise rotation about the O(11)–C(12) bond. Zero degrees is when the O(11)–C(12) bond is cisoid to and coplanar with the C(1)–C(2) bond.

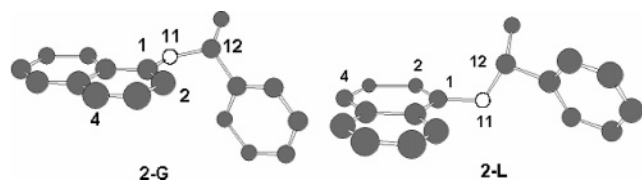


**FIGURE 3.** Calculated optimized ground-state geometries of the **2-G** and **2-L** conformations. The solid and open balls represent carbon and oxygen atoms, respectively. Hydrogen atoms have not been included for clarity.

tions at 25 °C that contain >97% of **2-G**. Given the caveats that the calculated energy differences may not be very accurate and that another local minimum of lower energy may have been missed, these data indicate that photochemistry originates from the **2-G** conformation; there is insufficient time within the short excited singlet lifetime of **2** (ca. 9.3 ns in hexane as determined by the time-correlated single-photon counting (TCSPC) technique) for an appreciable amount of **2-G** to reach the **2-L** conformation.

The structural differences of the **2-G** and **2-L** conformers in their  $S_0$  and  $S_1$  states are small. For instance, the C(2)–C(1)–O(11)–C(12) dihedral angle differs by only ca. 2–3°, and the O(11)–C(12) bond is lengthened very little despite its being cleaved to form radical-pair **B** and the adjacent C(1)–O(11) bond being shortened. We suspect

that significant O(11)–C(12) lengthening commences only after an associative  $n,\pi^*$  or  $\pi,\pi^*$  singlet state crosses to the dissociative  $\pi,\sigma^*$  state.<sup>8</sup>

## Discussion

**Irradiations of (*R*)-**2**. General Considerations.** The prochiral 1-phenylethyl radical of radical-pair **B** combines in-cage with the oxygen atom of its 1-naphthoxy radical partner (to generate the original (*R*)- or inverted (*S*)-enantiomer of **2**) or at C(2) and C(4) (to generate both enantiomers of long-lived keto intermediates that tautomerize<sup>22</sup> to **2BN** and **4BN**) (Scheme 2). In the absence of secondary photolytic reactions (vide ante), the stereoselectivity of the processes leading to **2BN** and **4BN** is established when the keto intermediates are formed. Alternatively, radicals of the initial pair may undergo in-cage disproportionation and hydrogen atom abstractions from surrounding chains or out-of-cage abstractions leading to **3–5**.<sup>7,23a</sup> Products that incorporate solvent and fragments of (*R*)-**1** or (*R*)-**2** are probably present,<sup>13a</sup> but we have not attempted to isolate or identify them because of their low yields. The sole source of **6**, however, must be out-of-cage combinations, and its presence serves as an indication that some **2**, **2BN**, and **4BN** are also formed out-of-cage (as racemic mixtures).<sup>7</sup> Regardless, the formation of products **3–5**, by either in-cage or out-of-cage reactions, has no influence on the subsequent kinetic analyses.<sup>24</sup>

The degree to which out-of-cage recombination reactions participate during irradiations of alkyl aryl ethers depends on the ability of solvent to scavenge radicals. Thus, chemically induced dynamic nuclear polarization (CIDNP) studies on 1,1-dimethylallyl 1-naphthyl ether and cyanomethyl 1-naphthyl ether in methanol, a good H-atom donor, give no evidence for out-of-cage formation of the Claisen products.<sup>25</sup> Cross-coupling experiments on photochemical rearrangements of allyl aryl ethers and diphenyl ethers, again in alcoholic solvents with easily abstractable H-atoms, indicate that the radical-pair combinations are only intracage.<sup>26</sup> However, involvement of some out-of-cage formation of rearrangement products is indicated when the solvents are poor H-atom donors.<sup>27</sup>

We infer when no **6** is detected upon irradiation of (*R*)-**1** or (*R*)-**2** that all of the **2**, **2BN**, and **4BN** derive from in-

(22) 1,3- and 1,5-H shifts for enolization of keto intermediates occur in the range of microseconds to seconds and depend strongly on the nature of the solvent. In fact, many of these tautomerisms are intermolecular. (a) Arai, T.; Tobita, S.; Shizuka, H. *J. Am. Chem. Soc.* **1995**, *117*, 3968–3975. (b) Chiang, Y.; Kresge, A. J.; Wirz, J. *J. Am. Chem. Soc.* **1984**, *106*, 6392–6395. (c) Chiang, Y.; Kresge, A. J.; Tang, Y. S.; Wirz, J. *J. Am. Chem. Soc.* **1984**, *106*, 460–462.

(23) (a) Nakagaki, R.; Hiramatsu, M.; Watanabe, T.; Tanimoto, Y.; Nagakura, S. *J. Phys. Chem.* **1985**, *89*, 3222–3226. (b)  $k \approx 1 \times 10^{11} \text{ s}^{-1}$  (ca. 10 ps) at 23 °C on the basis of the approximation that the rate constant doubles during each 10 °C increase in temperature.

(24) For convenience in deriving kinetic expressions and analyzing the data according to them, all products, except that fraction of **2**, **2BN**, and **4BN** from in-cage combinations, are attributed to cage-escape processes.

(25) (a) Pohlert, G.; Grimme, S.; Dreeskamp, H. *J. Photochem. Photobiol., A: Chem.* **1994**, *79*, 153–162. (b) Pohlert, G.; Dreeskamp, H.; Grimme, S. *J. Photochem. Photobiol., A: Chem.* **1996**, *95*, 41–49.

(26) (a) Kelly, D. P.; Pinhey, J. T.; Rigby, R. D. *Aust. J. Chem.* **1969**, *22*, 977–991. (b) Ogata, Y.; Takagi, K.; Ishino, I. *Tetrahedron* **1970**, *26*, 2703–2709. (c) Haga, N.; Takayanagi, H. *J. Org. Chem.* **1996**, *61*, 735–745.

(27) Galindo, F.; Miranda, M. A.; Tormos, R. *J. Photochem. Photobiol., A: Chem.* **1998**, *117*, 17–19 and references therein.

cage processes.<sup>7,10</sup> Statistically, the total amount of **2**, **2BN**, and **4BN** produced from out-of-cage processes is twice that of **6** since each of these molecules is constituted from two 1-phenylethyl radicals. The **2:2BN:4BN** product ratio from out-of-cage radical-pair **B** combinations during irradiations of (*R*)-**2** in liquid *n*-alkane solvents is assumed to be 1:1.4:4.0. This is the value from irradiations of (*R*)-**1** in hexane at 23 °C where virtually all of the radical-pair **B** combinations are assumed to be out-of-cage.<sup>7,10</sup> Justification<sup>7b</sup> for this assumption is based on the ca. 24-ns (at 23 °C) delay between formation of radical-pair **A** from (*R*)-**1** and its decarbonylation to generate radical-pair **B**.<sup>9</sup> Since small organic species can diffuse ca. 15 Å in 1 ns in a low viscosity solvent at room temperature,<sup>28</sup> there is ample opportunity for the components of radical-pair **A** to separate before decarbonylation of 2-phenylpropanoyl radicals. The in-cage yields and enantiomeric excesses from combinations of radical-pair **B** of (*R*)-**2** in Table 1 are calculated using these assumptions (see Supporting Information). We also assume that none of the reaction proceeds through the triplet manifold<sup>7c,8,10,11</sup> and that the in-cage yields of (*S*)-**2** are lower limits of the amounts of (*R*)-**2** generated from in-cage radical-pair **B** combinations since the initial orientation of a radical-pair **B** favors regeneration of (*R*)-**2**. Application of these assumptions and the data from in-cage combinations to the mechanism in Scheme 2 enable us to estimate the relative rate constants for the in-cage component of reaction.

**Combinations of Radical-Pairs A and B from Irradiations of (*R*)-1 and (*R*)-2 in Hexane.** Even in hexane, the photo-Fries rearrangement products from (*R*)-**1**, **2AN**, and **4AN** are from in-cage combinations.<sup>7,8</sup>

The radical center of 2-phenylpropanoyl is a localized sp<sup>2</sup> or p orbital while the radical character of 1-phenylethyl is delocalized throughout the π-system. In addition, the singly occupied sp<sup>2</sup> or p orbital is more electronegative than the benzylic radical. For these reasons, the 2-phenylpropanoyl radical is expected to be intrinsically more reactive toward other radicals, especially electron-rich ones, than the 1-phenylethyl radical.<sup>10,29,30</sup> Steric differences between the accessibility of the radical centers of 2-phenylpropanoyl and 1-phenylethyl must play a role as well, but they are not expected to be as important as the electronic factors, especially in low-viscosity liquid media.<sup>7,10</sup> As a result, in-cage combinations of the less selective 2-phenylpropanoyl radical with 1-naphthoxy tend to be less discriminating and more rapid. Being less reactive, the 1-phenylethyl radical is able to survey its options to a greater extent before adding to a position of a 1-naphthoxy radical. Thus, a larger fraction of combination events occurs in-cage at the more electron-rich (and, presumably, more reactive) C4 position<sup>13</sup> of the 1-naphthoxy radical. Consistent with this hypothesis, the

(**2AN/4AN**)<sub>in-cage</sub> ratios from (*R*)-**1** are much larger than the (**2BN/4BN**)<sub>in-cage</sub> ratios from (*R*)-**2**.<sup>31</sup> Radical-pair **A** retains partial memory of the structure of **1** (from which it emanated) than does radical-pair **B** when it is generated from **2**.<sup>7,12</sup>

The presence of **6** and lack of enantiomeric excess in the combination products from radical-pair **B** of (*R*)-**1** in hexane at room-temperature emphasize the influence of the ca. 24-ns “delay” before the appearance of prochiral 1-phenylethyl radicals,<sup>9</sup> and the opportunities which the delay provides for the components of radical-pair **A** to diffuse apart. Alternatively, it is possible that the 1-phenylethyl and 1-naphthoxy radicals tumble more rapidly than they combine, even when they are sequestered in a hexane cage. However, the lack of *ee* cannot be attributed to internal rotations about the phenyl-benzylic C–C bond of 1-phenylethyl because the activation energy, ca. 54 kJ/mol,<sup>32</sup> is too high to compete with combinations within a cage;<sup>1</sup> typically, ca. 12 kJ/mol is the activation energy for a diffusion-controlled radical–radical combination leading to a C–O bond.<sup>1</sup> On this basis, we ascribe the lack of significant *ee* in the decarbonylated products from (*R*)-**1** to their formation primarily from out-of-cage encounters that lead to reestablishment of radical-pairs **B**.

**Irradiations of (*R*)-2 in *n*-Alkanes at Different Temperatures. Dependence of Radical Movements on Solvent Properties.** In hexane, both the higher (**2BN/4BN**)<sub>total</sub> ratios and much higher *ees*<sub>total</sub> of **2BN** and **4BN** from irradiations of (*R*)-**2** than from irradiations of (*R*)-**1** indicate that radical-pairs **B** residing in the same cages where lysis of (*R*)-**2** occurred retain a significant memory of the structure of (*R*)-**2** at the time that they collapse to products. This assertion is supported by our quantum calculations that indicate a conformation very similar to the **2-G** ground state as the structure in the S<sub>1</sub> state where lysis occurs.<sup>33</sup> Thus, despite their intrinsic lower reactivity than 2-phenylpropanoyl radicals, 1-phenylethyl radicals produced directly from (*R*)-**2** as part of radical-pair **B** are able to react with their 1-naphthoxy radical partners in highly regio- and stereoselective fashions.

As mentioned, the 1-phenylethyl radical is “born” very near C(2) of 1-naphthoxy when (*R*)-**2** is irradiated. Thus, it is not surprising that *ee*<sub>2BN-in-cage</sub> > *ee*<sub>4BN-in-cage</sub>. This observation is not at odds with the oppositely ordered regioselectivities: **4BN**<sub>in-cage</sub> > **2BN**<sub>in-cage</sub> (Table 1). Higher stereoselectivity of prochiral radical-pair combinations requires faster combination rate constants, so that randomization from radical tumbling can be suppressed. The relative *ee* of the products is determined by the balance between the positional bias for attachment of a 1-phenylethyl radical to C(2) of 1-naphthoxy within an initial cage and the higher probability of bond formation for each collision near C(4) (because of its higher spin density).<sup>13</sup>

(28) A diffusion coefficient of ca. 10<sup>−5</sup> cm<sup>2</sup>/s is assumed.<sup>28a</sup> (a) Turro, N. J. *Pure Appl. Chem.* **1977**, *49*, 405–429.

(29) There are very few examples of direct comparisons of rates of reaction of different radicals with a common species. In one, *tert*-butyl radical reacted more rapidly than pivaloyl radical in 2-propanol with an electron-deficient partner, acrylonitrile.<sup>29a</sup> This is not a good test case for our work because the reactive partner here, 1-naphthoxy, is a relatively electron-rich radical. (a) Jent, F.; Paul, H.; Roduner, E.; Heming, M.; Fischer, H. *Int. J. Chem. Kinet.* **1986**, *18*, 1113–1122.

(30) Pryor, W. A. *Introduction to free radical chemistry*; Prentice Hall: Englewood Cliffs, NJ, 1966

(31) “Total” and “in-cage” values are exchangeable in some circumstances, including radical-pair **A** combinations in all of our media<sup>7,8</sup> and radical-pair **B** combinations in the solid phases of *n*-alkanes. The latter is inferred from the absence of product **6**.

(32) Conradi, M. S.; Zeldes, H.; Livingston, R. J. *Phys. Chem.* **1979**, *83*, 2160–2161.

(33) Interestingly, although lysis from a **2-G** or **2-L** conformer generates a prochiral radical-pair **B** in which the 1-phenylethyl radical resides above or below the plane of the 1-naphthoxy radical and, therefore, is disposed to add to one of its p-orbitals, the radical pair from **2-L** is oriented initially better to combine and yield a new photoproduct.

The intrinsic electronic properties of the radicals (N.B., their nucleophilicity and electrophilicity)<sup>30</sup> and their interactions with surrounding solvent molecules also influence the stereochemistry of the radical-pair combinations. For example, the absolute rate constants for formation of the keto intermediates of **2AN** and **4AN** are  $5 \times 10^8$  and  $4 \times 10^7$  s<sup>-1</sup>, respectively, at 23 °C during the photo-Fries reactions of **1** in an unstretched polyethylene film with 46% crystallinity, a highly constraining medium.<sup>7</sup> These values are more than 10-fold smaller than the rate constants in hexane, as estimated from the ca.  $k \approx 4 \times 10^{10}$  s<sup>-1</sup> rate for in-cage combination of 1-naphthoxy/acetyl singlet radical pairs in CH<sub>3</sub>CN at 10 °C.<sup>23</sup>

At the moment of its generation from (*R*)-**2**, radical-pair **B** has several options for reaction: (1) in-cage combination to regenerate **2** or to form **2BN** and **4BN** stereospecifically (i.e., without tumbling of the 1-phenylethyl radical); (2) in-cage combination with tumbling to form both (*S*)- and (*R*)-enantiomers of **2**, **2BN**, and **4BN**; and (3) diffusion of one of the radicals of the pair from its original solvent cage prior to in-cage combination. The probability that each will occur is dependent on the microviscosity that the location, flexibility, and electronic nature of neighboring solvent molecules impose on the radical pair and, therefore, on the rates of rotational (tumbling) and translational diffusion of the radicals within their cage.

As the length of an *n*-alkane increases, its bulk viscosity ( $\eta$ , used in Figure 2) does as well, resulting in retardation of radical movements and (not necessarily correlated) changes in the relative rates of the processes that determine which of the three options above is favored. For example, assuming that translational diffusion of a radical from its initial solvent cage is the motion most sensitive to solvent viscosity, the reciprocal of the fraction of in-cage combination of a radical pair can be expressed as a linear function of  $(1/\eta)^n$  (where  $n = 0.5$ –1.0 and  $1/\eta$  is defined as the solvent fluidity).<sup>1,34</sup> Although this expression does not always hold in solvents of low viscosity, like hexane,<sup>34f</sup> we find qualitatively that  $(2 \times (S)\text{-}2 + 2\text{BN} + 4\text{BN})_{\text{in-cage}}$ , the relative yield of in-cage radical-pair **B** combination products from irradiations of (*R*)-**2** (Table 1), increases with increasing viscosity. Since different motions of the radical pair are required to form **2BN** and **4BN**, they should be sensitive to  $\eta$  as well. A more quantitative analysis follows.

*Relative Rate Constants of Processes Associated with In-Cage Radical-Pair B Combinations.* The rate constant for a diffusion-controlled collision of two solutes (N.B., radicals in this case) through a solvent bulk,  $k_{\text{diff}}$ , can be estimated by the Smoluchowski equation,<sup>35</sup>

$$k_{\text{diff}} = 4\pi N'RD \quad (2)$$

where  $N'$  is  $10^{-3}$  of Avogadro's number,  $R$  is the sum of the collisional radii, and  $D$  is the sum of diffusion coefficients. For radical-pair **B**,  $R$  is ca. 5.5 Å because

$r_{1\text{-phenylethyl}} = 2.7$  Å and  $r_{1\text{-naphthoxy}} = 2.8$  Å assuming spherical shapes.

When the radius of the solute ( $r$ , assuming a spherical shape) is much larger than that of a solvent molecule, a linear relationship between  $D$  and solvent fluidity is predicted.<sup>36</sup> However, that is not the case here: the van der Waals volumes<sup>37</sup> of hexane, decane, tetradecane, and heptadecane (114, 182, 250, and 301 Å<sup>3</sup>, respectively) are near to or larger than those of 1-naphthoxy (124 Å<sup>3</sup>) and 1-phenylethyl (111 Å<sup>3</sup>). In this size regime, the radicals experience reduced microscopic frictional forces, and the velocities of their tumbling and translational motions are more accurately expressed by eq 3 using the microviscosity,  $\eta_m = f \times \eta$ ;  $f = D_{\text{SE}}/D_{\text{exptl}}$ .<sup>38,39</sup>  $f$  is the microfriction factor for translation<sup>40</sup> and the diffusion coefficients are calculated by the Stokes–Einstein equation ( $D_{\text{SE}}$ )<sup>36</sup> or measured experimentally ( $D_{\text{exptl}}$ ). In this way, the sum of the diffusion coefficients for the two components of radical-pair **B** is calculated to be  $8.7 \times 10^{-5}$  at 23 °C and  $1.3 \times 10^{-4}$  cm<sup>2</sup>/s at 60 °C in hexane. They and eq 2 lead to  $k_{\text{diff}} = 3.6 \times 10^{10}$  M<sup>-1</sup>s<sup>-1</sup> at 23 °C and  $5.4 \times 10^{10}$  M<sup>-1</sup>s<sup>-1</sup> at 60 °C. From Scheme 2, the ratio between the relative product yields (as percentages) from out-of-cage ( $100 \times (S)\text{-}2 + 2\text{BN} + 4\text{BN})_{\text{in-cage}}$  and in-cage ( $(2 \times (S)\text{-}2 + 2\text{BN} + 4\text{BN})_{\text{in-cage}}$ ) combinations can be expressed in terms of rate constants (eq 4).

$$D = kT/6\pi r\eta_m \quad (3)$$

$$100/(2 \times (S)\text{-}2 + 2\text{BN} + 4\text{BN})_{\text{in-cage}} - 1 = k_{\text{esc}}/(2k_2 + k_{2\text{BN}} + k_{4\text{BN}}) \quad (4)$$

Since  $k_{\text{esc}}$  is directly proportional to  $k_{\text{diff}}$ , the in-cage combination product yield can be related directly to the solvent microviscosity. The influence of solvent viscosity on the fates of the radical pairs is explored in Figure 4. Although the plots contain few points, their positive slopes indicate that the in-cage combination rate constants in eq 4 ( $k_2$ ,  $k_{2\text{BN}}$ , and  $k_{4\text{BN}}$ ) are less sensitive to microviscosity than is  $k_{\text{esc}}$  (vide ante). However, given the paucity of data points in each plot and the nature of the assumptions needed to derive eq 4, it is difficult to assess

(36) Einstein, A. *Investigations on the Theory of Brownian Motion*; Dover: New York, 1956.

(37) Bondi, A. *J. Phys. Chem.* **1964**, *68*, 441–451.

(38) (a) Kramers, H. A. *Physica* **1940**, *7*, 284–304. (b) Akesson, E.; Hakkaraianen, A.; Laitinen, E.; Helenius, V.; Gillbro, T.; Korppi-Tommola, J.; Sundstrom, V. *J. Chem. Phys.* **1991**, *95*, 6508–6523. (c) Ben-Amotz, D.; Drake, J. M. *J. Chem. Phys.* **1988**, *89*, 1019–1029. (d) Dote, J. L.; Kivelson, D.; Schwartz, R. N. *J. Phys. Chem.* **1981**, *85*, 2169–2180.

(39) (a) Sun, Y.; Saltiel, J. *J. Phys. Chem.* **1989**, *93*, 8310–8316. (b) Terazima, M.; Okamoto, K.; Hirota, N. *J. Chem. Phys.* **1995**, *102*, 2506–2515. (c) Kim, S. H.; Kim, S. K. *Bull. Korean Chem. Soc.* **1996**, *17*, 365–373.

(40) The microfriction factor for translation is defined as  $f = (0.16 + 0.4r_A/r_B)(0.9 + 0.4T_{rB} - 0.25T_{rA})$ .<sup>40a</sup>  $r_A$  and  $r_B$  are the radii of solute and solvent molecules, respectively, and can be estimated from their van der Waals volumes ( $V$ ; Å<sup>3</sup>) assuming the molecules are spherical ( $r = (3V/4\pi)^{1/3}$  where  $\chi = 0.74$  is the space-filling factor for closest-packed spheres);  $T_{rA}$  and  $T_{rB}$  are reduced temperatures of solute and solvent, respectively, and can be calculated from the equation  $T_r = (T - T_{\text{mp}})/(T_{\text{bp}} - T_{\text{mp}})$ , where  $T_{\text{mp}}$  and  $T_{\text{bp}}$  are melting and boiling points in Kelvin, respectively, of each molecule. In our case, ethylbenzene (van der Waals volume: 116 Å<sup>3</sup>; radius: 2.74 Å; melting point: 178.2 K; boiling point: 409.2 K) is used as a model for the 1-phenylethyl ( $r = 2.7$  Å) and 1-naphthoxy (2.8 Å) radicals to obtain the  $f$  values at 23 and 60 °C. More details are included in Supporting Information. (a) Spornol, A.; Wirtz, K. *Z. Naturforsch., A* **1953**, *8*, 522–532.

(34) (a) Koenig, T. *J. Am. Chem. Soc.* **1969**, *91*, 2558–2562. (b) Frisch, H. L.; Kuivila, H. G. *J. Am. Chem. Soc.* **1977**, *99*, 7200–7203. (c) Koenig, T.; Deinzer, M. *J. Am. Chem. Soc.* **1968**, *90*, 7014–7019. (d) Niki, E.; Kamiya, Y. *J. Am. Chem. Soc.* **1974**, *96*, 2129–2133. (e) Olea, A. F.; Thomas, J. K. *J. Am. Chem. Soc.* **1988**, *110*, 4494–4502. (f) Kiefer, H.; Traylor, T. G. *J. Am. Chem. Soc.* **1967**, *89*, 6667–6671.

(35) Smoluchowski, M. *V. Z. Phys. Chem.* **1917**, *92*, 129–168.

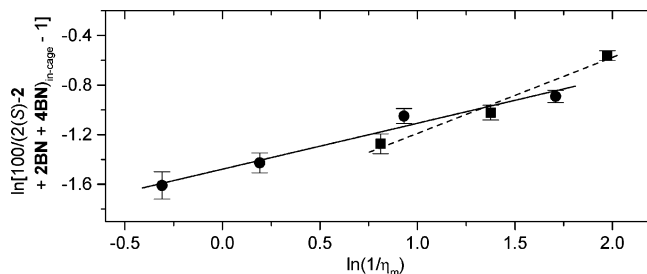
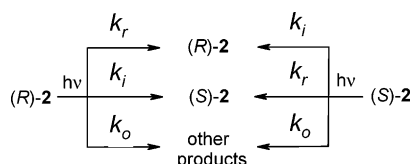


**FIGURE 4.** Plots of  $\ln[100/(2(S)-2 + 2BN + 4BN)_{\text{in-cage}} - 1]$  versus  $\ln(1/\eta_m)$  and the best linear fits for irradiations of (*R*)-**2** in various *n*-alkanes at 23 (●) and 60 °C (■).

### SCHEME 3. Photoreacemization of (*R*)-**2** in *n*-Alkanes



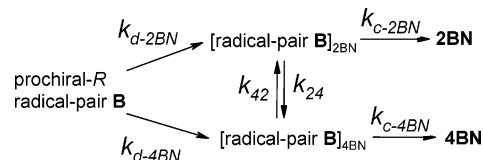
whether the values of the slopes at 23 °C ( $0.47 \pm 0.10$ ) and 60 °C ( $0.6 \pm 0.1$ ) for irradiations of (*R*)-**2** in the *n*-alkanes are truly different.

*Regio- and Stereoselectivities of In-Cage Radical-Pair B Combinations.* Qualitatively, the observation of high stereoselectivities of radical-pair **B** combinations during irradiations of (*R*)-**2** in *n*-alkanes requires that  $k_t$  (the in-cage tumbling rate constant of a 1-phenylethyl radical) be somewhat smaller than, but similar in magnitude to,  $k_{2BN}$ ,  $k_{4BN}$ , and  $k_{\text{esc}}$  (i.e., the rate constants involving some form of translational motion). This conclusion is supported by the low values of **S**, the probability that radical-pair **B** from irradiation of (*R*)-**2** will yield (*S*)-**2** (0.13–0.16; see eq 1), as well as analyses derived from them.

Given the nature of our reactive system, especially that the energies of the enantiomeric precursor radical-pairs **B** and their rate constants leading to (*R*)-**2** and (*S*)-**2** are the same,  $\mathbf{S} = 2P_{\text{inv}}/(1 - P_{\text{inv}} - P_{\text{ret}})$ , where  $P_{\text{inv}}$  and  $P_{\text{ret}}$  are the probabilities that radical-pair **B** combinations form the (*S*)- and (*R*)-enantiomers of **2**, respectively.<sup>17</sup> The expressions for  $P_{\text{inv}}$ ,  $P_{\text{ret}}$ , and **S** on the basis of Scheme 2 (see Supporting Information) are very complex and do not lend themselves to further analyses. However, on the basis of Scheme 3, a simplified form of Scheme 2 in which both prochiral radical-pair **B** species have been combined implicitly into one intermediate radical-pair **B** that is not shown,  $P_{\text{inv}} = k_i/(k_i + k_r + k_o)$  and  $P_{\text{ret}} = k_r/(k_i + k_r + k_o)$ . Thus,  $k_i \approx 0.07k_o$  in all of the *n*-alkane media investigated. Although the relationships among the rate constants in the two schemes are not direct,  $k_o$  is approximately  $k_{\text{esc}} + k_{2BN} + k_{4BN}$ , and  $k_i$  equals  $k_2$  multiplied by the fraction of prochiral-*R* radical-pair **B** that becomes prochiral-*S* radical-pair **B**. The constancy of the **S** values requires that changes of  $k_i$  caused by varying solvent viscosity or temperature (within the range investigated) are proportional to those suffered by the sum or the dominant term of ( $k_{\text{esc}} + k_{2BN} + k_{4BN}$ ).

Scheme 3 emphasizes the stereochemical aspects of the photoreactions of (*R*)-**2**. A related simplification of Scheme 2, Scheme 4, allows the regiochemical aspects of the kinetics to be investigated. In it, in-cage formation of **2BN**

### SCHEME 4. A Simplified Mechanism for In-Cage Radical-Pair B Combinations



and **4BN** is attributed to specific region-isomeric radical-pair **B** precursors, [radical-pair **B**]<sub>2BN</sub> and [radical-pair **B**]<sub>4BN</sub>. The derived eq 5 (see Supporting Information) can provide insights into the dependence of in-cage translational motions by the radicals (N.B.,  $k_{24}$ ,  $k_{42}$ ,  $k_{d-2BN}$ , and  $k_{d-4BN}$ ) on microviscosity.

$$(\mathbf{2BN}/\mathbf{4BN})_{\text{in-cage}} = k_{c-2BN}/k_{c-4BN} \times \frac{[(k_{42} + k_{c-4BN})k_{d-2BN} + k_{42}k_{d-4BN}]/[(k_{24} + k_{c-2BN})k_{d-4BN} + k_{24}k_{d-2BN}]}{\quad} \quad (5)$$

The rate constants for bond formation when a 1-phenylethyl radical is near C(2) and C(4) of 1-naphthoxy,  $k_{c-2BN}$  and  $k_{c-4BN}$ , are expected to be  $>10^{11} \text{ s}^{-1}$ ,<sup>23b</sup> they are dependent on the intrinsic electronic and steric properties of the radicals but not on the solvent microviscosities or electron spin changes. The viscosity-dependent rate constants for translational displacement of the radical-pair **B** components from their initial dispositions to the [radical-pair **B**]<sub>2BN</sub> and [radical-pair **B**]<sub>4BN</sub> orientations,  $k_{d-2BN}$  and  $k_{d-4BN}$ , should be smaller than  $k_{c-2BN}$  and  $k_{c-4BN}$ . The rate constants for interconversion of the two preproduct radical pairs,  $k_{24}$  and  $k_{42}$ , should be comparable to  $k_{d-2BN}$  and  $k_{d-4BN}$ . Thus,  $k_{d-2BN}$ ,  $k_{d-4BN}$ ,  $k_{24}$ , and  $k_{42}$  are expected to be the rate-limiting steps of the combination process. The slope of a plot of  $\ln(\mathbf{2BN}/\mathbf{4BN})_{\text{in-cage}}$  versus  $\ln(1/\eta_m)$  (Figure S4 of Supporting Information),  $-0.16 \pm 0.05$ , indicates that the in-cage combination process involving the longer pathway to **4BN** is influenced by microviscosity to a slightly greater extent than the shorter pathway to **2BN**.

Assuming that ca. 10-ps is required for radical-pair **B** from (*R*)-**2** to form the keto intermediate of **4BN** at 23 °C in hexane<sup>23b</sup> and an initial separation of 5.1 Å<sup>41</sup> between the benzylic radical center of 1-phenylethyl and the C(4) position of 1-naphthoxy after lysis of the C–O bond in (*R*)-**2**, an in-cage diffusion coefficient,  $D_{\text{in-cage}} \approx 1.3 \times 10^{-4} \text{ cm}^2/\text{s}$ , is calculated from eq 6.<sup>36,42</sup> It is in excellent agreement with the “macroscopic”  $D$  ( $=8.7 \times 10^{-5} \text{ cm}^2/\text{s}$ ) on the basis of eq 3.

$$d \approx (2Dt)^{1/2} \quad (6)$$

Furthermore, the extent of tumbling by 1-phenylethyl radicals along the pathways to C(2) and C(4) of their 1-naphthoxy partners are expressed in the (*S*)/(*R*) enan-

(41) The distance between the C(12) and O(11) nuclei in (*R*)-**2** is assumed to be the sum of their van der Waals radii, 3.22 Å, immediately after the ether bond breaks. Then, the minimum distance traveled by the reactive radical center of 1-phenylethyl to reach C(4) of 1-naphthoxy is estimated to be 5.1 Å based on a length for the newly formed C–O bond<sup>41a</sup> of 1.5 Å. (a) Allen, F. H.; Kennard, O.; Watson, D. G.; Brammer, L.; Orger, A. G.; Taylor, R. *J. Chem. Soc., Perkin Trans. 2* **1987**, S1–S19.

(42) Alwattar, A. H.; Lumb, M. D.; Birks, J. B. In *Organic Molecular Photochemistry*; Birks, J. B., Ed.; Wiley: New York, 1973; Vol. 2, pp 403–456.



tiomer ratios of the photoproducts. For the purposes of this discussion, we assume that no tumbling has occurred in those cases where a radical-pair **B** combination leads to the (*R*)-enantiomer of a product and that tumbling is the only route to an (*S*)-enantiomer.<sup>32</sup> Thus, the slopes of plots of  $\ln((S)\text{-}2\text{BN}/(R)\text{-}2\text{BN})_{\text{in-cage}}$  and  $\ln((S)\text{-}4\text{BN}/(R)\text{-}4\text{BN})_{\text{in-cage}}$  versus  $\ln(1/\eta_m)$  at 23 °C, both  $0.2 \pm 0.1$  (Figure S4 of Supporting Information), indicate that microviscosity influences  $k_t$ , the rate constant for tumbling of 1-phenylethyl radicals, to similar extents along the pathways leading to both **BN** products. As has been suggested,<sup>34,38</sup> no simple function can describe adequately the relationship between the fates of in-cage radical pairs and the properties of solvents.

## Conclusions

The regiochemistry and stereochemistry of photoproducts from irradiations of (*R*)-**2** and (*R*)-**1** have been analyzed to follow the motions of singlet radical pairs in their *n*-alkane cages. Significant stereoselectivity of prochiral radical-pair **B** combinations from photo-Claisen reactions of (*R*)-**2** has been observed even in the low-viscosity solvent, hexane, at room temperature. To achieve regio- and stereoselectivity in radical-pair recombination processes such as the ones investigated here, the prochiral radical pairs must be born with some orientational “memory” of their chiral parent molecules, and they must retain that memory throughout their lifetimes. Manifestations of these requirements are further demonstrated by the regio- and stereocourses of the reactions formally derived from prochiral singlet radical-pair **B** in *n*-alkanes of different viscosities. In addition, *quantitative* correlations between regio- or stereochemistries of the rearrangement photoproducts from (*R*)-**2** and solvent microviscosity provide interesting insights into how radical pairs move over short periods and distances when their confining cages have walls of varying flexibility. In that regard, both the regio- and stereoselectivities reach plateau values as the solvent viscosity increases, indicating that the relationships between the rates of radical-radical bond formation and either translational or tumbling motions within a solvent cage reach an asymptotic limit.

Overall, the results allow several basic motional processes by radical species, including translations within a cage, translational diffusion to escape from a cage, and tumbling within a cage, to be assessed in detail within small spaces for periods that approximate the reactive lifetimes. The probes and methodologies used to analyze their compartment should be applicable to investigation in a wide variety of other media, and future studies will be directed to that end.

## Experimental Section

**Instrumentation.** Melting points were corrected. Optical rotations were measured on a DigiPol DP781 polarimeter using a 10-cm cell. <sup>1</sup>H NMR spectra, referenced to internal TMS, were recorded on a Varian 300 MHz spectrometer. UV/vis absorption spectra were measured on a Cary 300 Bio UV-Visible Spectrophotometer. Gas chromatography (GC) was conducted on a Hewlett-Packard 5890 gas chromatograph equipped with a flame ionization detector. A 0.25- $\mu\text{m}$  DB-5 (0.25 mm  $\times$  30 m) column was used to check the purity of

products and monitor reactions. HPLC analyses were carried out on HP series 1100 liquid chromatograph equipped with an autosampler, a diode array detector, and a silica gel column (5  $\mu\text{m}$ , 4.6  $\times$  250 mm) for determinations of product distributions; or a semipreparative cyano column (5  $\mu\text{m}$ , 10  $\times$  250 mm) for product separations; or a Chiralcel OJ-H chiral column (Chiral Technologies Inc., 5  $\mu\text{m}$ , 4.6  $\times$  250 mm) for determinations of enantiomeric excesses (*ees*). Fluorescence decays of **2** were determined with an Edinburgh Analytical Instruments model FL900 time-correlated single photon counting (TCSPC) system using H<sub>2</sub> as the lamp gas. A hexane solution of  $10^{-5}$  M **2** in a quartz cuvette was degassed at  $<10^{-4}$  Torr. The principal decay component represents ca. 95% of the total counts for bi- or triexponential fits ( $\chi^2 \leq 1.2$ ) and the other decay components were found in weak emissions from the neat solvent.

**Materials.** The preparations of racemic **1** and **2** and photoproducts **2AN**, **4AN**, **2BN**, **4BN**, and **6**, as well as all reagents and solvents associated with them, have been reported previously.<sup>7,12</sup> *S*-(−)-1-Phenylethanol (97–99% *ee*) was purchased from Lancaster Synthesis, Inc. (*R*)-2-Phenylpropanoic acid (97+% *ee*) was obtained from TCI. Solvents for product analyses and separations were HPLC grade. All photoproducts were prepared and identified as reported previously.<sup>12</sup> (*R*)-**1**, mp 71.6–72.2 °C (lit.<sup>7b</sup> mp 51.2–53.3 °C for racemic **1**) and  $[\alpha]_D^{23} = -62.6^\circ$  (*c* 0.84, hexanes), was prepared in >99% chemical and enantio purity from reaction of 1-naphthol with (*R*)-2-phenylpropionic acid as described previously.<sup>12</sup>

(*R*)-**2** was prepared using Mitsunobu's method.<sup>43</sup> A 25-mL THF solution of 5.5 g (26.9 mmol) diisopropyl azodicarboxylate was added dropwise to 40 mL of an anhydrous THF solution of 1.95 g (13.5 mmol) 1-naphthol, 1.5 g (12.3 mmol) (*S*)-(−)-1-phenylethanol, and 6.4 g (24.5 mmol) PPh<sub>3</sub> under a N<sub>2</sub> atmosphere at ambient temperature. After ca. 36 h stirring, a white crystal (0.4 g; 15% yield; >99% chemical and enantio purity by HPLC), mp 67.4–68.1 °C (lit.<sup>7b</sup> mp 67.0–68.4 °C for racemic **2**) and  $[\alpha]_D^{23} = -264.5^\circ$  (*c* 0.4, hexanes), was obtained after column chromatography over silica gel using hexanes as eluent. <sup>1</sup>H NMR (CDCl<sub>3</sub>/TMS, 300 MHz): 6.64–8.45 ppm (m, 12H, aromatic), 5.51 ppm (quartet, 1H, −OCH(CH<sub>3</sub>)Ph, *J* = 6.3 Hz), 1.76 ppm (d, 3H, −OCH(CH<sub>3</sub>)Ph, *J* = 6.3 Hz). Mass: *m/z* calculated for C<sub>18</sub>H<sub>16</sub>O 248, found 248.

Hexane (puriss. p.a. ACS;  $\geq 99.5\%$  (GC)) was purchased from Fluka. Decane (99+% ) was from Aldrich. *n*-Tetradecane (99%) and *n*-heptadecane (99%) were purchased from Humphrey Chemical Company, North Haven, CT, and were used as received.

**General Procedure for Irradiations.** Deoxygenated (>45 min N<sub>2</sub> purging) solutions of 2 mM (*R*)-**1** or (*R*)-**2** in septum-sealed Pyrex tubes were irradiated with a 450 W Hanovia medium-pressure mercury lamp for between a few seconds and a few minutes at 23 °C. The time was varied empirically to obtain appropriate conversions. *n*-Dodecane and amylbenzene were used as internal standards for GC and HPLC analyses, respectively. Control of temperature ( $\pm 1$  °C) above 23 °C was achieved by immersing the sample tubes into a stirred water bath in a Pyrex beaker.

**Determination of Product Distributions and Enantiomeric Excesses.** An aliquot of each irradiated sample was analyzed directly using HPLC (silica column; mixture of hexanes and ethyl acetate as eluant) and GC to obtain the conversion and relative product distribution in which the relative yield of each product is shown by the percentage, and the sum of all photoproducts is 100%. See ref 12 for additional details. Analyses from at least three injections were averaged; the mass balance was always >80%.

The remainder of each irradiated sample was concentrated and the products were separated on a semipreparative HPLC column. Each separated chiral product was then dissolved in

(43) (a) Mitsunobu, O. *Synthesis* **1981**, 1–28. (b) Kometani, T.; Kondo, H.; Fujimori, Y. *Synthesis* **1988**, 1005–1007.

hexanes and analyzed by HPLC using a Chiralcel OJ-H column (mixture of hexanes and 2-propanol as eluant). The enantiomeric excess of each photoproduct or the remaining starting material was determined from the average peak area ratios of its (*R*) and (*S*) enantiomers at four different detection wavelengths with one or two injections. All of the HPLC peaks were homogeneous in that the shapes of their UV/vis absorption spectra were invariant throughout the peak widths.

**Quantum Mechanical Calculations.** All ab initio computations were performed using the Gaussian 98 package.<sup>44</sup> The optimized geometries in the ground state ( $S_0$ ) and first singlet excited state ( $S_1$ ) of **2** were obtained using the Hartree–Fock (HF) method and the configuration interaction singles approach (CIS) with the frozen core approximation,<sup>45</sup> respectively, at the level of 6-31G\* basis sets. Different initial geometries were used in the optimization processes to locate the global and local minima. In addition, harmonic frequencies of each optimized state were calculated to ensure that the obtained optimized geometry really corresponds to an energy minimum rather than a saddle point on the potential energy surface. The energy difference between the global and local minima in the ground state was obtained from calculations using the B3LYP/6-31G\* method, and the scale factor for the zero-point energy was 0.9804. The energy difference between the structures corresponding to the global and local minima in the first excited singlet state was calculated using the CIS/6-31G\* method.

**Acknowledgment.** The authors are grateful to the National Science Foundation for financial support of this research, to Prof. Tadashi Mori and to Prof. Miklos Kertesz and his research group for their assistance with the quantum mechanical calculations, and to Prof.

Christian Wolf for his advice concerning methods for determination of enantiomeric excesses and product separations. We thank the reviewers for several useful suggestions.

**Supporting Information Available:** Product distributions, enantiomeric excesses of (*R*)-**1** and (*R*)-**2**, extrapolations to 0% conversions from irradiations of (*R*)-**2**, definitions of  $P_{inv}$ ,  $P_{ret}$ , and **S** in terms of rate constants from Scheme 2, derivations of eq 5 and other eqs associated with Schemes 2–4, methods to obtain values in Table 1 and Figure 4, and data for *n*-alkanes and for geometry optimizations of **2** in its ground and first excited singlet states. This material is available free of charge via the Internet at <http://pubs.acs.org>.

JO048182T

(44) Frisch, M. J.; Trucks, G. W.; Schlegel, H. B.; Scuseria, G. E.; Robb, M. A.; Cheeseman, J. R.; Zakrzewski, V. G.; Montgomery, J. A. Jr.; Stratmann, R. E.; Burant, J. C.; Dapprich, S.; Millam, J. M.; Daniels, A. D.; Kudin, K. N.; Strain, M. C.; Farkas, O.; Tomasi, J.; Barone, V.; Cossi, M.; Cammi, R.; Mennucci, B.; Pomelli, C.; Adamo, C.; Clifford, S.; Ochterski, J.; Petersson, G. A.; Ayala, P. Y.; Cui, Q.; Morokuma, K.; Rega, N.; Salvador, P.; Dannenberg, J. J.; Malick, D. K.; Rabuck, A. D.; Raghavachari, K.; Foresman, J. B.; Cioslowski, J.; Ortiz, J. V.; Baboul, A. G.; Stefanov, B. B.; Liu, G.; Liashenko, A.; Piskorz, P.; Komaromi, I.; Gomperts, R.; Martin, R. L.; Fox, D. J.; Keith, T.; Al-Laham, M. A.; Peng, C. Y.; Nanayakkara, A.; Challacombe, M.; Gill, P. M. W.; Johnson, B.; Chen, W.; Wong, M. W.; Andres, J. L.; Gonzalez, C.; Head-Gordon, M.; Replogle, E. S.; Pople, J. A. *Gaussian 98*, Revision A.11.4; Gaussian: Pittsburgh, PA, 2002.

(45) (a) Foresman, J. B.; Head-Gordon, M.; Pople, J. A.; Frisch, M. *J. J. Phys. Chem.* **1992**, *96*, 135–149. (b) Foresman, J. B.; Schlegel, H. B. In *Recent Experimental and Computational Advances in Molecular Spectroscopy*; Fausto, R., Ed.; NATO-ASI Series C; Kluwer Academic: Amsterdam, The Netherlands, 1993.